High fat diet induces a microbiota-dependent increase in stem cell activity in the *Drosophila* intestine

Jakob von Frieling[1], Muhammed Naeem Faisal[1,3], Femke Sporn[1], Roxana Pfefferkorn[1], Felix Sommer[2], Philip Rosenstiel[2], Thomas Roeder[1,4#]

[1]Zoological Institute, Dept. Molecular Physiology, Kiel University, Kiel, Germany
[2]IKMB, UKSH, Kiel University, Kiel, Germany
[3]current address: University Faisalabad, Pakistan
[4]German Center for Lung Research, Airway Research Center North, Kiel, Germany

[#]Correspondence: Thomas Roeder, Zoological Institute, Dept. Molecular Physiology, Kiel University, Kiel, Germany, Tel.: ++49-431-8804181, Email: troeder@zoologie.uni-kiel.de

Abstract

High fat diets (HFDs) have been associated with several pathologies. Here we show that HFDs trigger the activation of intestinal stem cells in the *Drosophila* midgut. This induction of stem cell activation is transient and is preceded by induction of cytokine (upd3) expression in enterocytes. The presence of an indigenous microbiota is essential for the HFD-induced stem cell activation as this response is blunted in germ-free (GF) animals lacking a microbiota. Moreover, both the composition of the microbiota and bacterial load were markedly altered in response to chronic feeding of HFDs to the fly. On the host side, JNK signaling within the enterocytes was essential to transduce the effects of a HFD into substantial stem cell activation. Although the HFD-induced stem cell activity was only transient, a long lasting shaping of the cellular composition as seen by a substantially increased number of enteroendocrine cells was observed over long time periods. Taken together, HFD enhanced stem cell activities in the gut that completely relied on the presence of an indigenous microbiota and depended on JNK signaling within intestinal enterocytes.

Introduction

High caloric intake and especially high fat diets (HFD) are major causes of the epidemic development of obesity-associated diseases [1]. In addition to metabolically relevant organs, the intestine is particularly susceptible to the effects of a HFD, as it is in direct contact with the constituents of the diet. Consequently, nutritional interventions directly impact the intestinal structure and functionality [2]. A diet-dependent plasticity in size of the intestine has been reported[3], which comprises reduced intestinal sizes in response to dietary restriction[4] but also increased intestinal sizes following re-feeding after a period of starvation[5]. Structural changes in response to HFDs can be observed at different levels, ranging from subcellular structures in enterocytes [6] up to the cellular composition of the intestinal epithelium[7]. Especially the HFD induced effects on the structure of the intestine require tuning of the activity of intestinal stem cells (ISCs). In mammals, HFDs directly enhance activity of ISCs, leading to increased villi lengths in the small intestine; a reaction that involves ß-catenin signaling[8]. This HFD induced activation appears to be directly caused by the lipid content of the food [3, 9]. A recent study could show that confrontation with high lipid contents induces a very robust PPAR-δ activation in ISCs, thus enhancing the numbers of mitotically active cells in the intestine[9] [10]. Beside this adaptation to a highly energetic diet, this response also increases the tumorigenicity of intestinal progenitors[9] [2]. This observation correlates with epidemiological studies showing that different types of diets modulate the risk to develop intestinal cancers [11, 12], with high fat containing diets leading to higher prevalence for the development of colon cancers [13, 14]. Here, deregulated stem cell activities appear to be directly associated with alterations in intestinal JAK/STAT signaling[15].

Although major effects of HFDs on the stemness and tumorigenesis of ISC seem to be directly mediated by the confrontation of fat components with intestinal epithelial cells[9], secondary effects are also highly relevant for induction of the complex phenotype that results from chronic HFD consumption. One important link between HFDs and the development of diseases is the intestinal microbiota[16-18]. High fat dietary supplementation has been shown to alter the abundance, composition and physiological performance of the micobiota [19-21]. In flies, HFDs cause higher microbial abundances in the intestine [22]. Associations between altered or dysbiotic microbiota composition and metabolic diseases have been shown repeatedly[23, 24]. Furthermore, a causative role of

altered microbiota compositions for the development of metabolic disorders has clearly been shown by microbiota transfer experiments[25, 26]. In *Drosophila*, a link between a dysbiotic microbiota and the activity of stem cells in the intestine was shown [27]. Here, age associated increases in the abundance of peculiar microbial colonizer as well as infection with specific pathogens trigger activation of stem cell activities [28, 29].

Despite this large body of informative studies, our knowledge regarding the mechanisms by which HFDs regulate stem cell activity in the intestine is not comprehensive. Here, we use the fruit fly *Drosophila* as a model and show that HFD induces transient activation of stem cell activities via JNK-dependent activation of cytokine expression in enterocytes. This effect was clearly microbiota dependent. Thus, we suppose that HFDs exert their physiological effects not only directly through activation of stem cell by confrontation with different fat components, but also by indirect means encompassing alterations of the microbiota, especially of the amount of bacteria present in the intestine.

Results

We used the fruit fly *Drosophila melanogaster* as a model to study the effects of HFD on structural and physiological characteristics of the intestine. Furthermore, we analyzed the contribution of the microbiota for the induced phenotypical alterations. In addition to the well-known effects of HFD on major metabolic parameters, we focused our study on its effects on intestinal structure and physiology. Feeding on a HF diet triggered a burst of stem cell activity in the midgut (Fig. 1). Using flies that express GFP in the pattern of the escargot driver (esg), meaning expression restricted to intestinal stem cells (ISCs) and their direct descendants, the enteroblasts, we could show that short phases of HF dieting induced a substantial expansion of these cell types (Fig. 1B) if compared with untreated controls (Fig. 1A). A quantitative analysis of this reaction was done with animals that express luciferase in the same spatial pattern to allow for a quantitative cell mass estimation (Fig. 1C). Although only very short periods of HF dieting could elicit the response, a decline in the signal was observed over time (Fig. 1C). A similar pattern of cell number increases in response to HF diets was also detectable, if only enteroblasts were taken into account (Fig. 1D-F). Here, GFP was expressed in the pattern of the su(H)GBE-Gal4 driver. After three days, more enteroblasts could be detected (Fig. 1E) if compared with the matching controls (Fig. 1D). This was also seen after quantitative evaluation of

luciferase expression (Fig. 1F), and, similar as seen for the esg-specific signals (stem cells plus enteroblasts), an increase was still visible after 7 days of HD dieting. A direct evaluation of the effects of different diets on ISC activity was done by counting the numbers of phosphoH3 (pH3) positive cells in the gut, showing an increase in pH3 positive cells after 3 days of HF dieting (Fig. 1H), if compared with matching controls (Fig. 1G). Counting the numbers of pH3 positive cells revealed a statistically significantly different number of pH3 positive cells (Fig. 1I). To evaluate the effects of HFD on the cellular composition of the intestine, we counted the numbers of enteroendocrine cells, which are, similar as enterocytes, direct descendants of enteroblasts (Fig. 1K). This intervention led to a time dependent increase in their number (Fig. 1L), starting at day 5, peaking at day 7 and remaining for more than 2 weeks significantly different from the counts observed in animals subjected to a control diet.

JNK signaling is a major stress sensitive signaling pathway operative in the intestine. Therefore, we tested if HFD impacts the activation of JNK signaling (Fig. 2). In contrast to untreated controls (Fig. 2A), activated, meaning phosphorylated JNK (pJNK) was observed at higher levels in high fat treated animals (Fig. 2B). Furthermore, we used a JNK reporter line [30] (4xTRE-dsRed) and could show that the induced fluorescence in the anterior midgut was significantly higher in response to HFD compared to matching flies kept on a control die (Fig. 2C). A major target of JNK signaling in enterocytes is the cytokine upd3, which is directly linked to stem cell activation[31]. Thus, we quantified the effects of HFD on the expression of this cytokine. Using a reporter line (upd3-Gal4::UAS-GFP), we could show that, in comparisons with non treated animals (Fig. 2D), confrontation with a HFD increased the expression of *upd3* in enterocytes (Fig. 2E). Quantifying transcript levels of *upd3* by qRT-PCR showed a statistically significant increase in transcript abundance (Fig. 2F). To evaluate if HFD induced JNK activation is causally linked with upd3 activation, we tested if inhibition of JNK signaling by ectopic overexpression of a dominant negative basket allele (bsk^{DN}) in enterocytes has an impact on *upd3* expression. Flies expressing bsk^{DN} in enterocytes showed no increase in *upd3* expression in response to HF dieting (Fig. 2G), implying that activation of JNK by HF dieting is responsible for the increase in local *upd3* production and therewith responsible for stem cell activation. It is well established that upd3 produced by enterocytes is able to induce stem cell proliferation through activation of JAK/STAT signaling in ISCs. Therefore, we used a STAT reporter line indicates JAK/STAT pathway activation by

expression of GFP[32]. Cells with a stem cell-like appearance that are scatted throughout the intestine show signals in an anticipated pattern. The signal observed with these flies in the intestine is relative weak (Fig. 2H), whereas the corresponding signal is far stronger in animals subjected to HFD (Fig. 2I). A semi-quantitative evaluation of the fluorescence revealed a statistically significant increase in the signal strength (Fig. 2K).

The indigenous microbiota is known to be amenable to dietary interventions. Thus, we compared germ-free flies (GF) with those that have been reconstituted with a natural microbiota (Fig. 3). The latter type of reconstituted animals has been used for all previously described experiments. As already pointed out, feeding with a HF diet induced stem cell proliferation, visualized with *esg*-Gal4::UAS-GFP where ISCs and enteroblasts are labeled with GFP. In untreated controls reconstituted with a natural microbiota (RC), the number of *esg*-positive cells is relatively small (Fig. 3A) compared to those subjected to a HFD (Fig. 3B). In GF animals, untreated controls also display low amounts of *esg*-positive cells (Fig. 3C), similarly as those subjected to HFD (Fig. 3D). A quantitative evaluation of the numbers of *esg*-positive cells revealed the same information (Fig. 3E). This lack of induction was also observed in reporter strains that allow visualization of *upd3* expression (Fig. 3F-J) indicating that the signal that induces ISC proliferation is not present in GF animals. Whereas control animals reconstituted with a native microbiota showed low upd3-related signals (Fig. 3F), HFD induced a substantial increase in the signal (Fig. 3G). In germ free animals, both, untreated (Fig. 3H) and treated animals (Fig. 3I) show very low upd3-releate signals. Transcript quantification of upd3 in GF flies by qRT-PCR revealed a significant downregulation of transcript levels in response to HF diet as well as to control diet compared with animals carrying a functional microbiota (Fig. 3J).

To understand the effects of a HFD on the microbiota, we analyzed the compositions of the microbiota in response to the dietary conditions. HFD significantly altered the composition of the microbial community compared to the control diet, as illustrated by a separation in beta diversity using principal coordinate analysis based on unweighted UNIFRAC (Fig. 4A). Linear discriminant analysis effect size (LEfSe) revealed a significant increase of the orders Enterobacteriales and Caulobacterales upon HFD feeding. On the other hand, control flies showed an enrichment of species of the Lactobacillaceae family, especially from the *Pediococcus* genus (Fig. 4B). To examine, whether the observed alterations of the microbial community is sufficient to induce stem cell activity, we performed a fecal transplantation

assay (Fig. 4C-G). Therefore, we transferred the microbiota of either CD-fed or HFD-fed flies into GF flies, which express GFP in the pattern of the esg driver. Transfer of the CD microbiota had no effect on the number of esg-positive cells after 3 days (Fig. 4C) or 5 days (Fig. 4D). However, also transfer of the HFD microbiota showed no increase in the cell number on day 3 (Fig. 4E) or day 5 (Fig. 4F). A quantitative analysis of the esg-positive cells revealed that this intervention had no effect on stem cell activity in the intestine (Fig. 4 G), indicating that the altered composition of the microbiota does not seem to cause the increased stem cell activity seen under HFD feeding

In addition to the effect of HFD on the composition of the microbiota, we also observed a change in bacterial load. (Fig. 5). HFD feeding resulted in an approximately two times higher bacterial load in the intestines compared to CD (Fig.5A). Furthermore, HFD induced mild constipation, meaning that the number of fecal spots deposited in a defined time interval was reduced substantially. The reduction was about 60-70% in HFD-fed animals (Fig. 5B). GF animals also showed a reduced fecal spot production that was almost 50% lower compared to flies with reconstituted microbiota. In these flies, HF dieting reduced fecal spot production to a level that is also observed in reconstituted flies. Gut transit times appeared to depend on the diet, as CD-fed animals carrying a normal microbiota showed the shortest transit time, while HFD-fed animals had an increased transit time (Fig. 5C). This effect was further enhanced in GF animals. A widening of the intestinal diameter was observed in HFD-fed versus CD-fed animals (Fig.5 D&E), which could be an indicator for the increased bacterial mass in the intestine.

Discussion

High fat or lipid-rich diets are thought to be responsible for the development of a plethora of metabolic disorders including the epidemic increase in obesity and type2 diabetes. In the current study, we focused on the effects of lipid-rich diets on the intestine, which is the first organ that experiences this dietary intervention. Thus, we concentrated our efforts on the changes of the intestinal structure and physiology that are caused by this HFD using *Drosophila melanogaster* as a simple model. Here, feeding on a HFD induced a substantial increase in stem cell activities in the intestine, leading to altered cell numbers and changes in the cellular composition of this organ. This induced stem cell activation completely relied

on the presence of a functional intestinal microbiota. In germ free animals, no increase in stem cell activity could be observed. Moreover, we could show that this effect also depends on effective JNK signaling in enterocytes. We assume that the microbiota dependent signal is transduced in enterocytes via JNK signaling, finally leading to the production and release of the cytokine upd3. This, in turn, activates JAK/STAT signaling in ISCs and is thus essential for their induced proliferation. Taken together, HFD activated JNK signaling in enterocytes in a process that completely relied on the presence of the intestinal microbiota. Effects of lipid-rich diets on structural and functional characteristics of the intestine have been reported in several models. Interestingly, different mechanisms appear to be operative in transducing lipid-rich diets into changes of proliferative activities of stem cells. In *Drosophila*, diets with very high cholesterol concentrations increased the abundance of enteroendocrine cells significantly. This was due to a direct interaction with Notch-signaling leading to a preference of enteroendocrine cell production [7]. Here, reducing the lipid amount was able to reduce the proliferative characteristics of enteroendocrine tumor formation. In mice, HFD induced comparable effects that are mainly characterized by increased proliferative activities in intestine[33-35]. Beyaz and colleagues [9, 10] found that HFD induced the stemness of intestinal stem cells, which was accompanied by a decoupling of the stem cell activity from its niche. This reaction is opposite to the augmented stem-cell function observed in response to dietary restriction in the intestine that depends on a more effective integration into the stem cell niche rather than from its decoupling [4]. Comparable to the effects caused by cholesterol in the *Drosophila* intestine, the HFD induced effects can be traced back to the direct interaction between peculiar fatty acids the ISC [10].

These stemness promoting effects of lipid-rich diets are caused by direct interactions between specific compounds of these diets (cholesterol or fatty acids) and cells of the intestine. This is in contrast to the mechanism of stemness promoting effects of HFDs in our system, which is indirect, as it always requires the presence of the microbiota. Lipid-rich diets have been associated with the occurrence of a dysbiotic microbiota, which have been causally linked with the occurrence of various pathogenic states. These dysbiotic states of the microbiota are also observed during aging [27, 28]. Most studies focused on the composition of the microbiota, meaning that shift towards specific bacterial colonizers correlate with the potential to foster pathogenic situations in the host. This appears not to

be relevant in the *Drosophila* system, as fecal transfer experiments failed to recapitulate the enhanced stemness phenotype. Instead, an increase in its abundance of bacterial colonizers appears to be more relevant. Two different factors most likely contribute to higher abundances of the microbiota in response to HFD; the high energy content that fosters growth of bacteria within the intestine, and increased gut transit times leading to reduced fecal output thus reducing loss of bacteria. In flies, an increased gut transit time and a reduced fecal output was observed, which might indeed be most important for the diet induced increase in microbial abundances. These increased gut transit times in response to HFD are also seen in mice and humans [36-38], indicating that it represents a general response type towards this type of nutritional intervention and that HFD is usually associated with increased bacterial abundances. One simple result of this increased abundance would be a higher pressure within the intestinal lumen, leading to higher pressures within this structure. This would open an additional avenue to explain the HFD induced increases of the stemness of ISC, namely a pressure induced activation of stem cell activities in the intestine [39]. Here, the so-called piezo channel in precursors of enteroendocrine cells responds to mechanical stress with the production of novel enteroendocrine cells, which is in line with the results of this study. We could also show that JNK signaling in enterocytes is essential to translate these stressful information into a suited cellular response[40, 41]. This sentinel function of enterocytes is highly relevant, because these cells are confronted with a plethora of stressful signals and have to signal their actual state in order to enable their replacement if necessary[42, 43].

In addition to the effects of lipid-rich diets on the stem cell activity in the intestine, we also realized that long-lasting modifications of the intestine's hormonal architecture are induced by this intervention. Feeding on a lipid-rich diet increased the number of enteroendocrine cells for a considerable time period. This observation is consistent with earlier reports showing that HFD has multiple effects on gut function and homeostasis[44] and that it leads to changes in the expression and release of gut hormones[45]. These gut hormones take a central position in metabolic control and regulate various aspects of gut function[46]. Based on our results the possibility cannot be ruled out that even a relatively short episode of lipid-rich dieting reorganizes the intestinal homeostasis for long periods. In mammals, substantial and long lasting effects of short episodes of lipid-rich dieting (e.g. only 3d) attenuated major lipid sensing systems operative in the gut [47]. Usually, intake of lipid-rich

diets reduce appetite via a hormonal circuitry[48] to effectively prevent overnutrition[49]. Whereas almost nothing is known regarding the effects of lipid-rich diets on gut hormone release in *Drosophila*, a plethora of studies shows this relationship in different mammals[50, 51]. Chronic exposure to high-fat diets in rats induced an increased release of CCK s one of the major gut hormones [52]. Similar effects have been reported for other gut hormones such as glp-1 [53], but the nature of this increased release remains to be elucidated. Few interventions have been shown to trigger changes of the number of enteroendocrine cells in the intestine[54]. Changing the number of enteroendocrine cell would not only modify the hormonal and metabolic homeostasis of the animal, it may also change the stem cell niche, as these cells are highly relevant for maintaining this important niche[55].

Taken together, our results clearly show that periods of lipid-rich dieting have major effects on the intestinal structure and function even in the simple model organism *Drosophila melanogaster*. These reactions comprise the transient activation of stem cell activity and the long lasting change of the cellular architecture of the gut. Moreover, we could show that this highly interesting and relevant reaction completely depends on the presence of a microbiota. The stress sensing JNK signaling pathway appears to be of central importance in transducing these effects.

Acknowledgements

We would like to thank Britta Laubenstein and Christiane Sandberg for excellent technical help. Moreover, we would like to thank Michelle Markstein, Erika Bach, Norbert Perrimon, Stephen Hou, Chris Wegner, and the Bloomington Stock center for flies. This work was supported by the German Research Foundation as part of the CRC 1182 (subproject C2) and the cluster of excellence Inflammation@Interfaces.

Material and Methods

Fly food and husbandry

All flies were raised in vials on sterile standard cornmeal medium containing 5 % inactivated yeast (BD Bacto™ yeast extract), 8,6 % cornmeal (Mühle Schlingemann, Waltrop,

Germany), 5 % glucose (Roth, Karlsruhe, Germany) and 1 % agar-agar (Roth) in an incubator at 20 °C and 65 % humidity. 3-5 days after hatching, adult flies were transferred on fresh sterile standard cornmeal medium or high fat medium. The high fat medium was made of the same components in identical concentrations, except that it contained 20 % (w/v) food-grade palm fat (Palmin®). The following fly strains were used in this study: w^{1118} (Bloomington Stock Center), *esg-GFP* (gift from N. Perrimon, Harvard University, USA), amon-Gal4 (gift from C. Wegener, Würzburg, Germany), *UAS-Luc* (gift from M. Markstein, University of Massachusetts, USA), *su(H)GBE-Gal4* (gift from S. Hou, Frederick, USA) *UAS-basket*^{DN} (Bloomington Stock Center 44801), *10XSTAT::GFP* (E. Bach, New York, USA), *20xUAS-IVS-mCD8::GFP* (Bloomington Stock Center 32194), and 4XTRE-DsRed (Bloomington Stock Center 59011).

Axenic flies

Flies were allowed to lay eggs on apple juice agar plates containing 2 % agar-agar (Roth 5210.2), and 50 % apple juice (Rewe Bio appe juice) for about 12 hours at 25 °C to prevent the presence of larvae. Eggs were collected by rinsing the apple juice agar plates with deionized water and were transferred into net baskets. Afterwards, the eggs were bleached for 2 min with 6 % sodiumhypochlorid (Roth, Karlsruhe, Germany) followed by washing steps with 70 % ethanol (Roth) and double autoclaved water under sterile conditions. The bleached embryos were then placed on sterile standard cornmeal medium. Emerged adults were tested for the lack of bacteria by PCR using universal primers for bacterial 16S rDNA.

Reconstitution with bacteria

A mixture of the following bacterial species was used for reconstitution of a natural microbiota that were cultured as previously described (Leitão-Conçalves et al., 2017): *Acetobacter pomorum* (OD_{600} = 0.7), *Lactobacillus brevis*^{EW} (OD_{600} = 8), *Lactobacilles plantarum*^{WJL} (OD_{600} = 6), *Enterococcus faecalis* (OD_{600} = 0.8) and *Commensalibacter intestini*^{A911T} (OD_{600} = 1.5) (kindly provided by Carlos Ribeiro, Lisbon, Portugal). To prepare the stock solution for recolonization, the following volumes of each liquid culture were combined in a 15 ml falcon tube: 2 ml of *A. pomorum*, 0.02 ml of *L. brevis*^{EW}, 0.25 ml of *L. plantarum*^{WJL}, 2 ml *E. faecalis* and 1 ml *C. intestini*^{A911T}. The bacterial mixture was centrifuged three times at 3.000 rpm for 15 min and repeatedly resuspended in sterile PBS. Finally, the

mixture was centrifuged at 3.000 rpm for 15 min and was resuspended in 25 % glycerol in sterile PBS. Aliquots of 500 µl were stored at -20 °C. A volume of 50 µl of the bacterial mixture was added to the surface of the control media or the high fat media and allowed to settle for 1 h at room temperature under sterile conditions. Afterwards, 3-5 day old germ-free flies were transferred to the corresponding media.

Fecal transplantation

3-5 day old reconstituted *esg*-GFP flies were cultured on high fat or control diet for 7 days. Subsequently, 5 flies were homogenized in 300 µl MRS medium (BD Difco™, Thermo Scientific, Braunschweig, Germany) by using a bead mill Ruptor 24 (BioLab Products, Bebensee, Germany). The fly debris was removed by centrifugation and the supernatant was mixed with 5 % sucrose. 200 µl of the mix was applied on a sterile filter paper. GF *esg*-GFP flies were allowed to feed on the filter paper for 24h. Afterwards, the flies were transferred to a control diet for 5 or 7 days. The GFP-positive cells were counted in the anterior midgut region.

Body fat quantification

Total body triacylglycerols (TAGs) in flies were determined using a coupled colorimetric assay (CCA) method as describes previously (Hildebrandt et al., 2011; Hoffmann et al., 2013). Groups of 5 females were weighed and homogenized in 1 ml 0.05 % Tween-20 using a Bead Ruptor 24 (BioLab Products, Bebensee, Germany). Homogenates were heat-inactivated at 70 °C for 5 min, centrifuged, and incubated with triglyceride solution (Thermo Fisher Scientific, Braunschweig, Germany) at 37 °C for 30 min. Glyceryl trioleate was used to prepare a standard curve. Absorbances were measured at 562 nm.

Immunohistochemistry

The intestines were dissected in PBS and subsequently fixed in 4 % paraformaldehyde for 1 h at room temperature. The intestines were washed 3 times with PBST (0.1 % Triton X-100 in PBS) and blocked in blocking buffer (5 % normal goat serum in PBST) for 1 h at room temperature. Afterwards, the intestines were incubated with the primary antibody in blocking buffer overnight at 4°C. Then, after three washing steps, the intestines were incubated with the secondary antibody in PBST at 4 °C overnight in darkness.

Subsequently, the intestines were washed three times with PBST and mounted on slides in Mowiol 40-88. Images were obtained using a fluorescence microscope equipped with an Apotome (Carl Zeiss Image Axio Vision). The following antibodies were used: anti-prospero from mouse (1:50, DSHB MR1A), anti-GFP from mouse (1:300, DSHB 8H11), anti-active JNK pAb from rabbit (Promega), AlexaFluor 488-labelled goat anti-mouse IgG (1:300, Jackson ImmunoResearch) and AlexaFlour 555-conjugated goat anti-mouse IgG (1:300, Cell Signaling Technology).

Fluorescence quantification of the *in vivo* stat-GFP reporter

Intestines of 10xSTAT::GFP flies were dissected 3 days after control dieting or HFD. The intestines were immediatly fixed in 4% PFA followed by 3 washing steps with PBT 0,1%. All images were stacked with 2 µm thickness and an exposure time of 60 ms. The fluorescence of all cells in the field of view were measured by using ImageJ. The corrected total cell fluorescence (CTCF) was calculated as followed: CTCF = integrated density – (area of selected cell x mean fluorescence of backround readings.

Luciferase assay

The luciferase assay was performed as previously described (Markstein et al., 2008) with minor modifications. The intestines of 5 adult flies per replicate were collected in 150 µl Glo Lysis Buffer (Promega, #E2661, Mannheim, Germany) and homogenized using a bead mill homogenizer (BioLab Products, Bebensee, Germany) for 2 min at 3.25 m/s. The homogenate was transferred to new reaction tubes and stored at -20 °C until further processing. For luciferase measurement samples were thawed on ice and 50 µl were transferred to a white 96-well plate with flat, white bottom with at least one empty well between treatments. The samples were mixed with the same amount of substrate provided by the One Glo Luciferase Assay System (Promega, #E6110, Mannheim, Germany) right before signal detection. Luciferase signal was detected using a Tecan plate reader (Tecan, Infinite M200 Pro, Männedorf, Switzerland). A defined control was used on every plate to normalize treatments across plates.

Fecal output

A small chunk of control diet or HF diet supplemented with Brilliant Blue FCF food dye (E133, Ruth, Bochum, Germany) were transferred on the bottom of a vial. A coverslip was placed in the middle of the vial, that it splits the vial in two halves. Individual flies were trapped on one half, together with the chunk of fly flood and the vial were plugged with a foam plug. The flies were then incubated at 20 °C for 24h. The coverslips with the defecation spots were scanned. The numbers of fecal spots were counted manually.

Intestinal transit time

The wells of 24-well plates were each loaded with a small chunk of either control diet or HF diet supplemented with Brilliant Blue FCF food dye. Individual flies were starved for 24 h, afterwards they were transferred to the wells and monitored every 15 min for 3 h. The appearance of the first dyed fecal spot determined the time from food ingestion to egestion per individual fly, which is referred to as transit time.

RNA extraction and quantitative RT-PCR

Total RNA was extracted from the midgut of adult female flies, which were kept on standard cornmeal medium or high fat medium. Quantitative RT-PCR was performed as described previously [56]. The following primers were used: *upd3* forward (5′-GAGAACACCTGCAATCTGAA-3′), *upd3* reverse (5′- AGAGTCTTGGTGCTCACTGT-3′) and for the quantification of the bacterial load: 8FM (5′-AGAGTTTGATCMTGGCTCAG-3′), Bact515R (5′-TTACCGCGGCKGCTGGCAC-3′).

16S amplicon sequencing

DNA was isolated from intestines containing fecal material using the DNeasy Blood and Tissue Kit (Qiagen) following the manufacturer's protocol for purification of total DNA from animal tissues and for pretreatment for gram-positive bacteria. Intestines of 10 individual flies were pooled for one sample to generate sufficient material. Extracted DNA was eluted from the spin filter silica membrane with 100 µl of elution buffer and stored at -80 °C.

16S profiling and MiSeq sequencing was performed as described earlier [57, 58] with the following modifications: the V3-V4 region of the 16S gene was amplified using the dual

barcoded primers 341F (GTGCCAGCMGCCGCGGTAA) and 806R (GGACTACHVGGGTWTCTAAT). Each primer contained additional sequences for a 12 base Golay barcode, Illumina adaptor and a linker sequence [59]. PCR was performed using the Phusion Hot Start Flex 2X Master Mix (NEB) in a GeneAmp PCR system 9700 (Applied Biosystems) and the following program [98°C for 3 min, 30x (98°C for 20 s, 55°C for 30 s, 72°C for 45 s), 72°C for 10 min, hold at 4°C]. Performance of the PCR reactions was checked using agarose gel electrophoresis. Normalization was performed using the SequalPrep Normalization Plate Kit (Thermo Fisher Scientific, Darmstadt, Germany) following the manufacturer's instructions. Equal volumes of SequalPrep-normalized amplicons were pooled and sequenced on an Illumina MiSeq (2 x 300 nt).

MiSeq sequence data was analyzed using MacQIIME v1.9.1 [60]. Briefly, all sequencing reads were trimmed keeping only nucleotides with a Phred quality score of at least 20, then paired-end assembled and mapped onto the different samples using the barcode information. Rarefaction was performed at 34,000 reads per sample to normalize all samples to the minimum shared read count and to account for differential sequencing depth. Sequences were assigned to operational taxonomic units (OTUs) using uclust and the greengenes reference database (gg_13_8 release) with 97% identity. Representative OTUs were picked and taxonomy assigned using uclust and the greengenes database. Quality filtering was performed by removing chimeric sequences using ChimeraSlayer and by removing singletons and sequences that failed to align with PyNAST. The reference phylogenetic tree was constructed using FastTree 2. Relative abundance was calculated by dividing the number of reads for an OTU by the total number of sequences in the sample. Unweighted Unifrac beta diversity was calculated and visualized by principal coordinate plots. Differentially abundant taxa were assessed using nonparametric t test and p values

were adjusted for multiple testing using FDR correction. Linear discriminant analysis (LDA) effect size (LEfSe) [61] was performed using the online tool available at http://huttenhower.sph.harvard.edu/galaxy. LDA denotes taxa based on their contribution to the overall observed differences between groups, i.e. taxa being significantly increased in abundance in HFD compared to CD diet.

Statistical Analysis

All analysis were performed with Prism 6.0 (GraphPad Software). Lifespan data were analyzed by log rank test (Mantel cox).

1. Ogden CL, Yanovski SZ, Carroll MD, Flegal KM. The epidemiology of obesity. Gastroenterology. 2007;132(6):2087-102. doi: 10.1053/j.gastro.2007.03.052. PubMed PMID: 17498505.
2. Alonso S, Yilmaz OH. Nutritional Regulation of Intestinal Stem Cells. Annu Rev Nutr. 2018;38:273-301. doi: 10.1146/annurev-nutr-082117-051644. PubMed PMID: 29799767.
3. Haller S, Jasper H. You Are What You Eat: Linking High-Fat Diet to Stem Cell Dysfunction and Tumorigenesis. Cell Stem Cell. 2016;18(5):564-6. doi: 10.1016/j.stem.2016.04.010. PubMed PMID: 27152439.
4. Yilmaz OH, Katajisto P, Lamming DW, Gultekin Y, Bauer-Rowe KE, Sengupta S, et al. mTORC1 in the Paneth cell niche couples intestinal stem-cell function to calorie intake. Nature. 2012;486(7404):490-5. doi: 10.1038/nature11163. PubMed PMID: 22722868; PubMed Central PMCID: PMCPMC3387287.
5. O'Brien LE, Soliman SS, Li X, Bilder D. Altered modes of stem cell division drive adaptive intestinal growth. Cell. 2011;147(3):603-14. doi: 10.1016/j.cell.2011.08.048. PubMed PMID: 22036568; PubMed Central PMCID: PMCPMC3246009.
6. Zeituni EM, Wilson MH, Zheng X, Iglesias PA, Sepanski MA, Siddiqi MA, et al. Endoplasmic Reticulum Lipid Flux Influences Enterocyte Nuclear Morphology and Lipid-dependent Transcriptional Responses. J Biol Chem. 2016;291(45):23804-16. doi: 10.1074/jbc.M116.749358. PubMed PMID: 27655916; PubMed Central PMCID: PMCPMC5095432.
7. Obniski R, Sieber M, Spradling AC. Dietary Lipids Modulate Notch Signaling and Influence Adult Intestinal Development and Metabolism in Drosophila. Dev Cell. 2018;47(1):98-111 e5. doi: 10.1016/j.devcel.2018.08.013. PubMed PMID: 30220569.
8. Mao J, Hu X, Xiao Y, Yang C, Ding Y, Hou N, et al. Overnutrition stimulates intestinal epithelium proliferation through beta-catenin signaling in obese mice. Diabetes. 2013;62(11):3736-46. doi: 10.2337/db13-0035. PubMed PMID: 23884889; PubMed Central PMCID: PMCPMC3806619.
9. Beyaz S, Yilmaz OH. Molecular Pathways: Dietary Regulation of Stemness and Tumor Initiation by the PPAR-delta Pathway. Clin Cancer Res. 2016;22(23):5636-41. doi:

10.1158/1078-0432.CCR-16-0775. PubMed PMID: 27702819; PubMed Central PMCID: PMCPMC5135602.
10. Beyaz S, Mana MD, Roper J, Kedrin D, Saadatpour A, Hong SJ, et al. High-fat diet enhances stemness and tumorigenicity of intestinal progenitors. Nature. 2016;531(7592):53-8. doi: 10.1038/nature17173. PubMed PMID: 26935695; PubMed Central PMCID: PMCPMC4846772.
11. Nystrom M, Mutanen M. Diet and epigenetics in colon cancer. World J Gastroenterol. 2009;15(3):257-63. PubMed PMID: 19140224; PubMed Central PMCID: PMCPMC2653321.
12. Reddy BS. Types and amount of dietary fat and colon cancer risk: Prevention by omega-3 fatty acid-rich diets. Environ Health Prev Med. 2002;7(3):95-102. doi: 10.1265/ehpm.2002.95. PubMed PMID: 21432290; PubMed Central PMCID: PMCPMC2723490.
13. Newmark HL, Yang K, Lipkin M, Kopelovich L, Liu Y, Fan K, et al. A Western-style diet induces benign and malignant neoplasms in the colon of normal C57Bl/6 mice. Carcinogenesis. 2001;22(11):1871-5. PubMed PMID: 11698351.
14. Ning Y, Wang L, Giovannucci EL. A quantitative analysis of body mass index and colorectal cancer: findings from 56 observational studies. Obes Rev. 2010;11(1):19-30. doi: 10.1111/j.1467-789X.2009.00613.x. PubMed PMID: 19538439.
15. Karunanithi S, Levi L, DeVecchio J, Karagkounis G, Reizes O, Lathia JD, et al. RBP4-STRA6 Pathway Drives Cancer Stem Cell Maintenance and Mediates High-Fat Diet-Induced Colon Carcinogenesis. Stem Cell Reports. 2017;9(2):438-50. doi: 10.1016/j.stemcr.2017.06.002. PubMed PMID: 28689994; PubMed Central PMCID: PMCPMC5549806.
16. Cani PD, Bibiloni R, Knauf C, Waget A, Neyrinck AM, Delzenne NM, et al. Changes in gut microbiota control metabolic endotoxemia-induced inflammation in high-fat diet-induced obesity and diabetes in mice. Diabetes. 2008;57(6):1470-81. doi: 10.2337/db07-1403. PubMed PMID: 18305141.
17. Cani PD, Neyrinck AM, Fava F, Knauf C, Burcelin RG, Tuohy KM, et al. Selective increases of bifidobacteria in gut microflora improve high-fat-diet-induced diabetes in mice through a mechanism associated with endotoxaemia. Diabetologia. 2007;50(11):2374-83. doi: 10.1007/s00125-007-0791-0. PubMed PMID: 17823788.
18. Hildebrandt MA, Hoffmann C, Sherrill-Mix SA, Keilbaugh SA, Hamady M, Chen YY, et al. High-fat diet determines the composition of the murine gut microbiome independently of obesity. Gastroenterology. 2009;137(5):1716-24 e1-2. doi: 10.1053/j.gastro.2009.08.042. PubMed PMID: 19706296; PubMed Central PMCID: PMCPMC2770164.
19. Kim KA, Gu W, Lee IA, Joh EH, Kim DH. High fat diet-induced gut microbiota exacerbates inflammation and obesity in mice via the TLR4 signaling pathway. PLoS One. 2012;7(10):e47713. doi: 10.1371/journal.pone.0047713. PubMed PMID: 23091640; PubMed Central PMCID: PMCPMC3473013.
20. de La Serre CB, Ellis CL, Lee J, Hartman AL, Rutledge JC, Raybould HE. Propensity to high-fat diet-induced obesity in rats is associated with changes in the gut microbiota and gut inflammation. Am J Physiol Gastrointest Liver Physiol. 2010;299(2):G440-8. doi: 10.1152/ajpgi.00098.2010. PubMed PMID: 20508158; PubMed Central PMCID: PMCPMC2928532.
21. Daniel H, Gholami AM, Berry D, Desmarchelier C, Hahne H, Loh G, et al. High-fat diet alters gut microbiota physiology in mice. ISME J. 2014;8(2):295-308. doi: 10.1038/ismej.2013.155. PubMed PMID: 24030595; PubMed Central PMCID: PMCPMC3906816.

22. Fink C, Staubach F, Kuenzel S, Baines JF, Roeder T. Noninvasive analysis of microbiome dynamics in the fruit fly Drosophila melanogaster. Appl Environ Microbiol. 2013;79(22):6984-8. doi: 10.1128/AEM.01903-13. PubMed PMID: 24014528; PubMed Central PMCID: PMCPMC3811555.
23. Li X, Watanabe K, Kimura I. Gut Microbiota Dysbiosis Drives and Implies Novel Therapeutic Strategies for Diabetes Mellitus and Related Metabolic Diseases. Front Immunol. 2017;8:1882. doi: 10.3389/fimmu.2017.01882. PubMed PMID: 29326727; PubMed Central PMCID: PMCPMC5742320.
24. Tilg H, Moschen AR. Microbiota and diabetes: an evolving relationship. Gut. 2014;63(9):1513-21. doi: 10.1136/gutjnl-2014-306928. PubMed PMID: 24833634.
25. Backhed F, Ding H, Wang T, Hooper LV, Koh GY, Nagy A, et al. The gut microbiota as an environmental factor that regulates fat storage. Proc Natl Acad Sci U S A. 2004;101(44):15718-23. doi: 10.1073/pnas.0407076101. PubMed PMID: 15505215; PubMed Central PMCID: PMCPMC524219.
26. Turnbaugh PJ, Ley RE, Mahowald MA, Magrini V, Mardis ER, Gordon JI. An obesity-associated gut microbiome with increased capacity for energy harvest. Nature. 2006;444(7122):1027-31. doi: 10.1038/nature05414. PubMed PMID: 17183312.
27. Guo L, Karpac J, Tran SL, Jasper H. PGRP-SC2 promotes gut immune homeostasis to limit commensal dysbiosis and extend lifespan. Cell. 2014;156(1-2):109-22. doi: 10.1016/j.cell.2013.12.018. PubMed PMID: 24439372; PubMed Central PMCID: PMCPMC3928474.
28. Buchon N, Broderick NA, Chakrabarti S, Lemaitre B. Invasive and indigenous microbiota impact intestinal stem cell activity through multiple pathways in Drosophila. Genes Dev. 2009;23(19):2333-44. doi: 10.1101/gad.1827009. PubMed PMID: 19797770; PubMed Central PMCID: PMCPMC2758745.
29. Buchon N, Broderick NA, Poidevin M, Pradervand S, Lemaitre B. Drosophila intestinal response to bacterial infection: activation of host defense and stem cell proliferation. Cell Host Microbe. 2009;5(2):200-11. doi: 10.1016/j.chom.2009.01.003. PubMed PMID: 19218090.
30. Chatterjee N, Bohmann D. A versatile PhiC31 based reporter system for measuring AP-1 and Nrf2 signaling in Drosophila and in tissue culture. PLoS One. 2012;7(4):e34063. doi: 10.1371/journal.pone.0034063. PubMed PMID: 22509270; PubMed Central PMCID: PMCPMC3324472.
31. Chakrabarti S, Dudzic JP, Li X, Collas EJ, Boquete JP, Lemaitre B. Remote Control of Intestinal Stem Cell Activity by Haemocytes in Drosophila. PLoS Genet. 2016;12(5):e1006089. doi: 10.1371/journal.pgen.1006089. PubMed PMID: 27231872; PubMed Central PMCID: PMCPMC4883764.
32. Bach EA, Ekas LA, Ayala-Camargo A, Flaherty MS, Lee H, Perrimon N, et al. GFP reporters detect the activation of the Drosophila JAK/STAT pathway in vivo. Gene Expr Patterns. 2007;7(3):323-31. doi: 10.1016/j.modgep.2006.08.003. PubMed PMID: 17008134.
33. Singh A, Balint JA, Edmonds RH, Rodgers JB. Adaptive changes of the rat small intestine in response to a high fat diet. Biochim Biophys Acta. 1972;260(4):708-15. PubMed PMID: 5028118.
34. Sagher FA, Dodge JA, Johnston CF, Shaw C, Buchanan KD, Carr KE. Rat small intestinal morphology and tissue regulatory peptides: effects of high dietary fat. Br J Nutr. 1991;65(1):21-8. PubMed PMID: 1705145.

35. Balint JA, Fried MB, Imai C. Ileal uptake of oleic acid: evidence for adaptive response to high fat feeding. Am J Clin Nutr. 1980;33(11):2276-80. doi: 10.1093/ajcn/33.11.2276. PubMed PMID: 7435405.
36. Anitha M, Reichardt F, Tabatabavakili S, Nezami BG, Chassaing B, Mwangi S, et al. Intestinal dysbiosis contributes to the delayed gastrointestinal transit in high-fat diet fed mice. Cell Mol Gastroenterol Hepatol. 2016;2(3):328-39. doi: 10.1016/j.jcmgh.2015.12.008. PubMed PMID: 27446985; PubMed Central PMCID: PMCPMC4945127.
37. vd Baan-Slootweg OH, Liem O, Bekkali N, van Aalderen WM, Rijcken TH, Di Lorenzo C, et al. Constipation and colonic transit times in children with morbid obesity. J Pediatr Gastroenterol Nutr. 2011;52(4):442-5. doi: 10.1097/MPG.0b013e3181ef8e3c. PubMed PMID: 21240026.
38. Taba Taba Vakili S, Nezami BG, Shetty A, Chetty VK, Srinivasan S. Association of high dietary saturated fat intake and uncontrolled diabetes with constipation: evidence from the National Health and Nutrition Examination Survey. Neurogastroenterol Motil. 2015;27(10):1389-97. doi: 10.1111/nmo.12630. PubMed PMID: 26176421; PubMed Central PMCID: PMCPMC4584183.
39. He L, Si G, Huang J, Samuel ADT, Perrimon N. Mechanical regulation of stem-cell differentiation by the stretch-activated Piezo channel. Nature. 2018;555(7694):103-6. doi: 10.1038/nature25744. PubMed PMID: 29414942; PubMed Central PMCID: PMCPMC6101000.
40. Wu H, Wang MC, Bohmann D. JNK protects Drosophila from oxidative stress by trancriptionally activating autophagy. Mech Dev. 2009;126(8-9):624-37. doi: 10.1016/j.mod.2009.06.1082. PubMed PMID: 19540338; PubMed Central PMCID: PMCPMC2750887.
41. Stronach BE, Perrimon N. Stress signaling in Drosophila. Oncogene. 1999;18(45):6172-82. doi: 10.1038/sj.onc.1203125. PubMed PMID: 10557109.
42. Zhou F, Rasmussen A, Lee S, Agaisse H. The UPD3 cytokine couples environmental challenge and intestinal stem cell division through modulation of JAK/STAT signaling in the stem cell microenvironment. Dev Biol. 2013;373(2):383-93. doi: 10.1016/j.ydbio.2012.10.023. PubMed PMID: 23110761; PubMed Central PMCID: PMCPMC3534909.
43. Gervais L, Bardin AJ. Tissue homeostasis and aging: new insight from the fly intestine. Curr Opin Cell Biol. 2017;48:97-105. doi: 10.1016/j.ceb.2017.06.005. PubMed PMID: 28719867.
44. Little TJ, Horowitz M, Feinle-Bisset C. Modulation by high-fat diets of gastrointestinal function and hormones associated with the regulation of energy intake: implications for the pathophysiology of obesity. Am J Clin Nutr. 2007;86(3):531-41. PubMed PMID: 17823414.
45. Richards P, Pais R, Habib AM, Brighton CA, Yeo GS, Reimann F, et al. High fat diet impairs the function of glucagon-like peptide-1 producing L-cells. Peptides. 2016;77:21-7. doi: 10.1016/j.peptides.2015.06.006. PubMed PMID: 26145551; PubMed Central PMCID: PMCPMC4788507.
46. Murphy KG, Bloom SR. Gut hormones and the regulation of energy homeostasis. Nature. 2006;444(7121):854-9. doi: 10.1038/nature05484. PubMed PMID: 17167473.
47. Cheung GW, Kokorovic A, Lam CK, Chari M, Lam TK. Intestinal cholecystokinin controls glucose production through a neuronal network. Cell Metab. 2009;10(2):99-109. doi: 10.1016/j.cmet.2009.07.005. PubMed PMID: 19656488.
48. Gillum MP, Zhang D, Zhang XM, Erion DM, Jamison RA, Choi C, et al. N-acylphosphatidylethanolamine, a gut- derived circulating factor induced by fat ingestion,

inhibits food intake. Cell. 2008;135(5):813-24. doi: 10.1016/j.cell.2008.10.043. PubMed PMID: 19041747; PubMed Central PMCID: PMCPMC2643061.
49. El-Salhy M, Mazzawi T, Gundersen D, Hatlebakk JG, Hausken T. Changes in the symptom pattern and the densities of large-intestinal endocrine cells following Campylobacter infection in irritable bowel syndrome: a case report. BMC Res Notes. 2013;6:391. doi: 10.1186/1756-0500-6-391. PubMed PMID: 24073715; PubMed Central PMCID: PMCPMC3849659.
50. Pilichiewicz AN, Little TJ, Brennan IM, Meyer JH, Wishart JM, Otto B, et al. Effects of load, and duration, of duodenal lipid on antropyloroduodenal motility, plasma CCK and PYY, and energy intake in healthy men. Am J Physiol Regul Integr Comp Physiol. 2006;290(3):R668-77. doi: 10.1152/ajpregu.00606.2005. PubMed PMID: 16210415.
51. Feinle-Bisset C, Patterson M, Ghatei MA, Bloom SR, Horowitz M. Fat digestion is required for suppression of ghrelin and stimulation of peptide YY and pancreatic polypeptide secretion by intraduodenal lipid. Am J Physiol Endocrinol Metab. 2005;289(6):E948-53. doi: 10.1152/ajpendo.00220.2005. PubMed PMID: 15998659.
52. Spannagel AW, Nakano I, Tawil T, Chey WY, Liddle RA, Green GM. Adaptation to fat markedly increases pancreatic secretory response to intraduodenal fat in rats. Am J Physiol. 1996;270(1 Pt 1):G128-35. doi: 10.1152/ajpgi.1996.270.1.G128. PubMed PMID: 8772510.
53. van Citters GW, Kabir M, Kim SP, Mittelman SD, Dea MK, Brubaker PL, et al. Elevated glucagon-like peptide-1-(7-36)-amide, but not glucose, associated with hyperinsulinemic compensation for fat feeding. J Clin Endocrinol Metab. 2002;87(11):5191-8. doi: 10.1210/jc.2002-020002. PubMed PMID: 12414891.
54. Worthington JJ. The intestinal immunoendocrine axis: novel cross-talk between enteroendocrine cells and the immune system during infection and inflammatory disease. Biochem Soc Trans. 2015;43(4):727-33. doi: 10.1042/BST20150090. PubMed PMID: 26551720; PubMed Central PMCID: PMCPMC4613519.
55. Scopelliti A, Cordero JB, Diao F, Strathdee K, White BH, Sansom OJ, et al. Local control of intestinal stem cell homeostasis by enteroendocrine cells in the adult Drosophila midgut. Curr Biol. 2014;24(11):1199-211. doi: 10.1016/j.cub.2014.04.007. PubMed PMID: 24814146; PubMed Central PMCID: PMCPMC4046228.
56. Warmbold C, Uliczka K, Rus F, Suck R, Petersen A, Silverman N, et al. Dermatophagoides pteronyssinus major allergen 1 activates the innate immune response of the fruit fly Drosophila melanogaster. J Immunol. 2013;190(1):366-71. Epub 2012/12/04. doi: 10.4049/jimmunol.1201347. PubMed PMID: 23203927.
57. Sommer F, Adam N, Johansson MEV, Xia L, Hansson GC, Bäckhed F. Altered Mucus Glycosylation in Core 1 O-Glycan-Deficient Mice Affects Microbiota Composition and Intestinal Architecture. PLoS One. 2014;9(1):e85254.
58. Sommer F, Ståhlman M, Ilkayeva O, Arnemo Jon M, Kindberg J, Josefsson J, et al. The Gut Microbiota Modulates Energy Metabolism in the Hibernating Brown Bear Ursus arctos. Cell Reports. 2016;14(7):1655-61. doi: 10.1016/j.celrep.2016.01.026.
59. Caporaso JG, Lauber CL, Walters WA, Berg-Lyons D, Huntley J, Fierer N, et al. Ultra-high-throughput microbial community analysis on the Illumina HiSeq and MiSeq platforms. ISME J. 2012;6(8):1621-4. doi: 10.1038/ismej.2012.8. PubMed PMID: 22402401; PubMed Central PMCID: PMCPMC3400413.
60. http://www.wernerlab.org/software/macqiime.
61. Segata N, Izard J, Waldron L, Gevers D, Miropolsky L, Garrett WS, et al. Metagenomic biomarker discovery and explanation. Genome biology. 2011;12(6):R60. doi: 10.1186/gb-2011-12-6-r60. PubMed PMID: 21702898; PubMed Central PMCID: PMCPMC3218848.

Figures

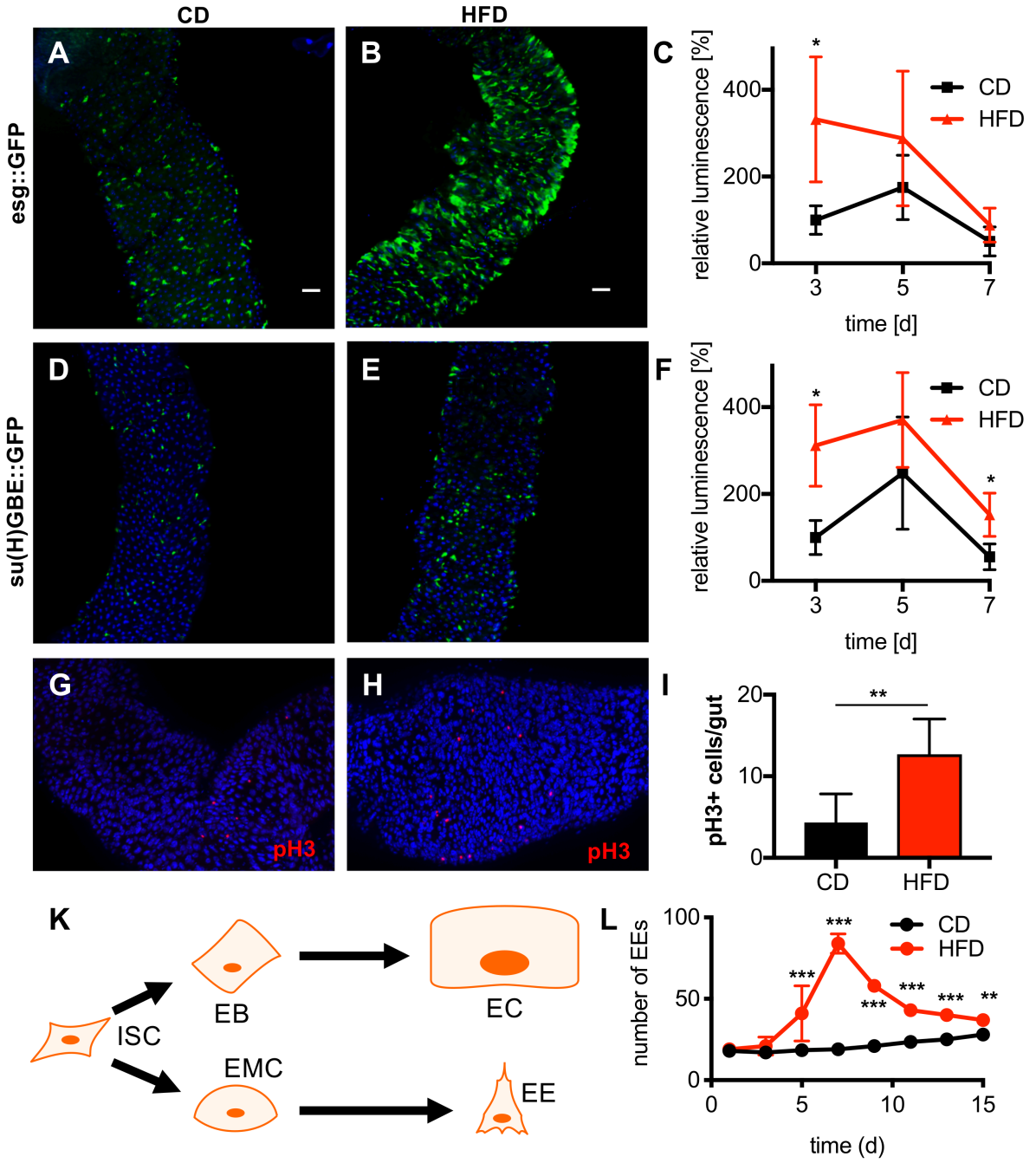

Figure 1: Impact of a high fat diet on the cell composition of the *Drosophila* intestine. Intestines (anterior midgut (AM) R2 region) of animals with labeled intestinal stem cells and enteroblasts (*esg-Gal4::UAS-GFP*) kept on a control diet (A) or subjected for 3 days to a HFD (B) are shown. (C) Luciferase signal of esg$^+$ cells ectopically expressing luciferase (*esg-Gal4::UAS-luciferase*). The intestines were dissected 3, 5 and 7 days after high fat or control diets (n=9-14). (D-E) Pattern of GFP expressed under the control of the enteroblast-specific *su(H)GBE* driver (*su(H)GBE-Gal4::UAS-mCD8-GFP*) driver. In (D) control animals are shown, whereas (E) shows the intestine of an animal subjected to HFD. (F) Quantification of luciferase signals of su(H)GBE$^+$ cells in response to either control or HFD. Representative images of anti-pH3 staining in the R4 region intestines of female flies kept on control diet (G)

or on HFD (H). (I) Quantification of the numbers of anti-pH3 positive cells in whole intestines (n = 6). (K) Scheme of the cell types of the *Drosophila* midgut, ISC = intestinal stem cell, EB = enteroblast, EC = enterocyte, EMC, enteroendocrine mother cell, EE, enteroendocrine cell. (L) Enteroendocrine (EEC) cell counts in the R2 region of the intestines over 15 days of high fat or control diet (n = 10). For all images, DAPI was used as a counterstain (scale bar = 50 µm). CD = control diet, HFD = high fat diet, *p>0.05, **p>0.01, ***p>0.001, ns = not significant.

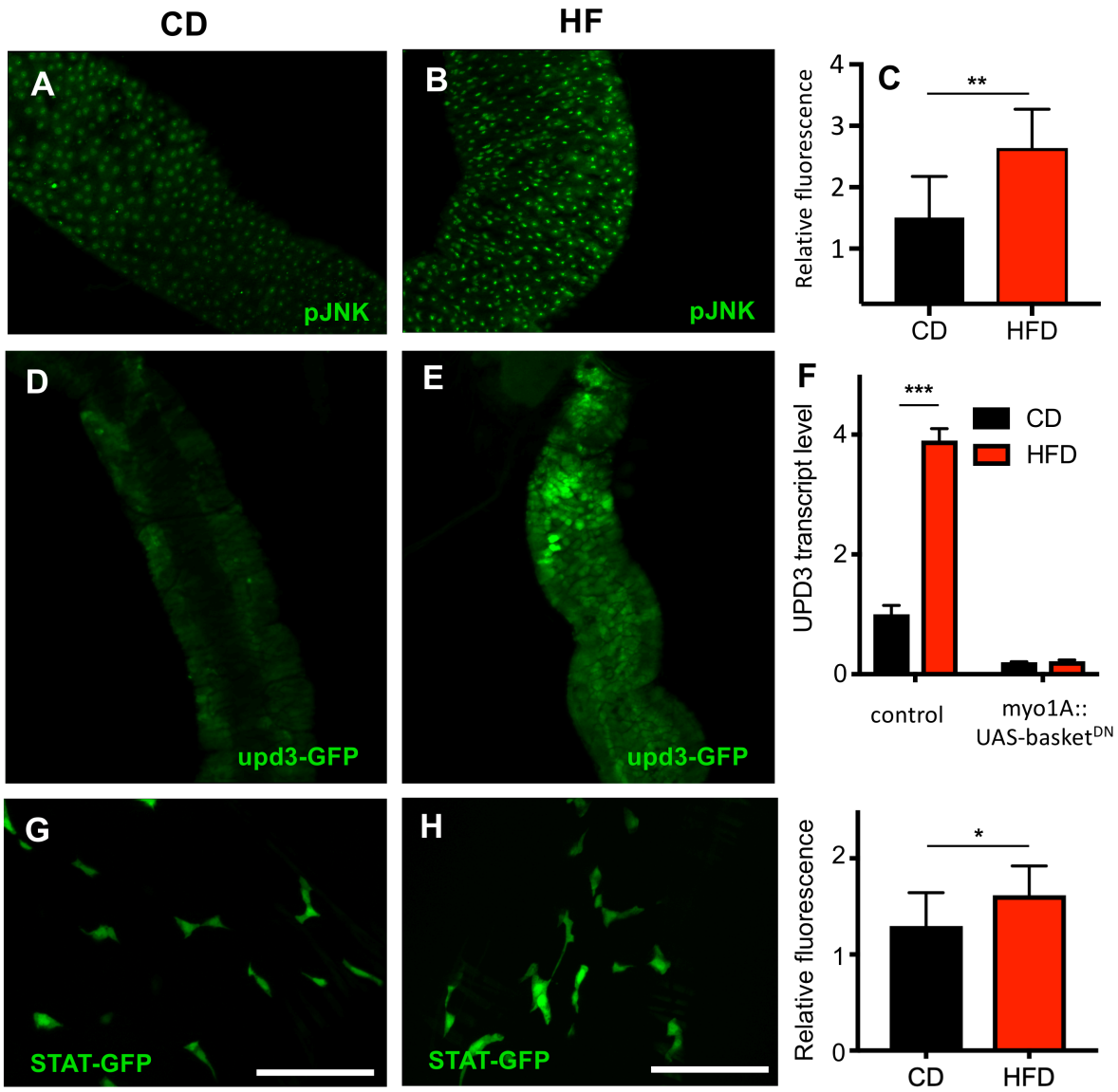

Figure 2. High fat diet induces *upd3* expression via JNK signaling. Anti-phospho JNK antibody staining of intestines of control animals and those subjected to 3 d of HFD (B) (scale bar = 50 µm). A JNK reporter line (4XTRE-DsRed) was subjected to HFD and fluorescence of anterior midguts were recorded (n=5, C). An *upd3-GFP in vivo* reporter was used to monitor upd3 expression in the intestine of control flies (D) and those kept for 3 d on a HFD (E). Representative images of the anterior midgut R2 region of the intestines are shown (scale bar = 50 µm). (F) qRT-PCR analysis of *upd3* transcription in the intestine of female w^{1118} flies fed with a HFD or control diet for 3 days (n = 5). (G) qRT-PCR analysis of *upd3* transcription in intestines expressing a dominant-negative form of basket in enterocytes (*myo1A-Gal4::UAS-basket*^{DN}) compared to the responder control (w^{1118}*::UAS-basket*^{DN}) (n = 5). Images of intestines isolated from a *STAT-GFP in vivo* reporter strain of animals on control (H) and on HFD (I). (K) Quantification of the fluorescence signal of the *STAT-GFP* reporter line after 3 days of HFD or control diet (n=10). CD RC = control diet recolonized, HFD RC = high fat diet recolonized, *p>0.05, ***p>0.001, ns = not significant.

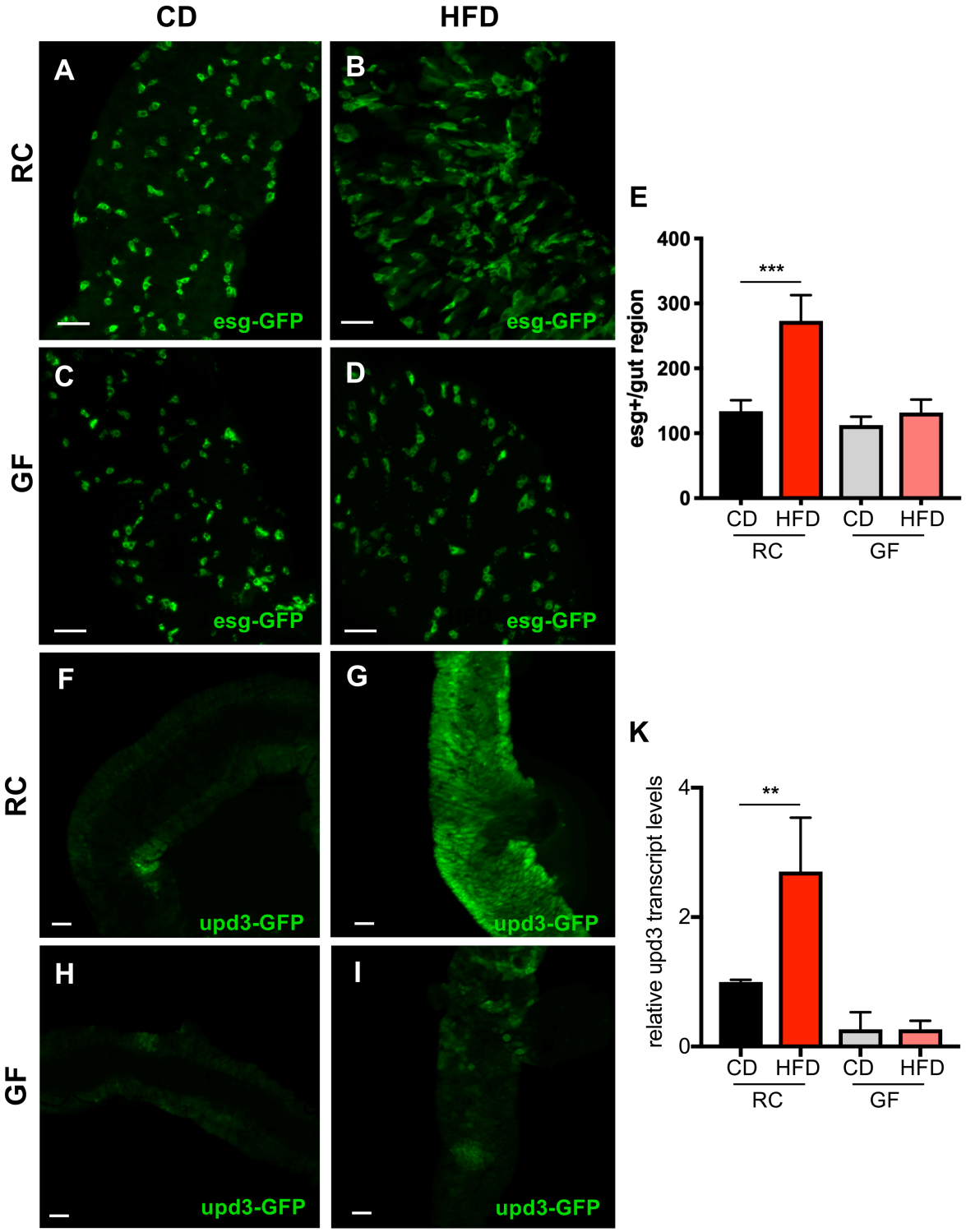

Figure 3. Impact of the intestinal microbiota on high fat diet induced cell proliferation and upd3 expression. Animals of the genotype (*esg-Gal4::UAS-GFP*) that label intestinal stem cells and enteroblasts, with a normal, reconstituted microbiota (A, B) kept on control diet (A) or on HFD (B). Germ free flies (C, D) kept on control (C) or HFD (D) (representative images of the anterior midgut (AM) R2 region of the intestines are shown (scale bar = 50 µm)). (E) Cell number measurement of *esg*$^{+}$ cells in the R2 region of the corresponding intestines (n=10). (F-I) An *upd3-GFP* reporter was used to examine the microbiota-associated modulation of upd3 expression. Animals with a normal microbiota (F, G) subjected to control (F) or HFD (G).

Germ-free flies (H, I), kept on control (H) or HFD (I) (representative images of the R2 region are shown (scale bar = 50µm). (J) qRT-PCR analysis of *upd3* transcripts in germ-free and recolonized flies fed with either control diet or HFD (n=5). CD RC = control diet recolonized, HFD RC = high fat diet recolonized, CD GF = control diet germ-free, HFD GF = high fat diet germ-free, *p>0.05, ***p>0.001, ns = not significant.

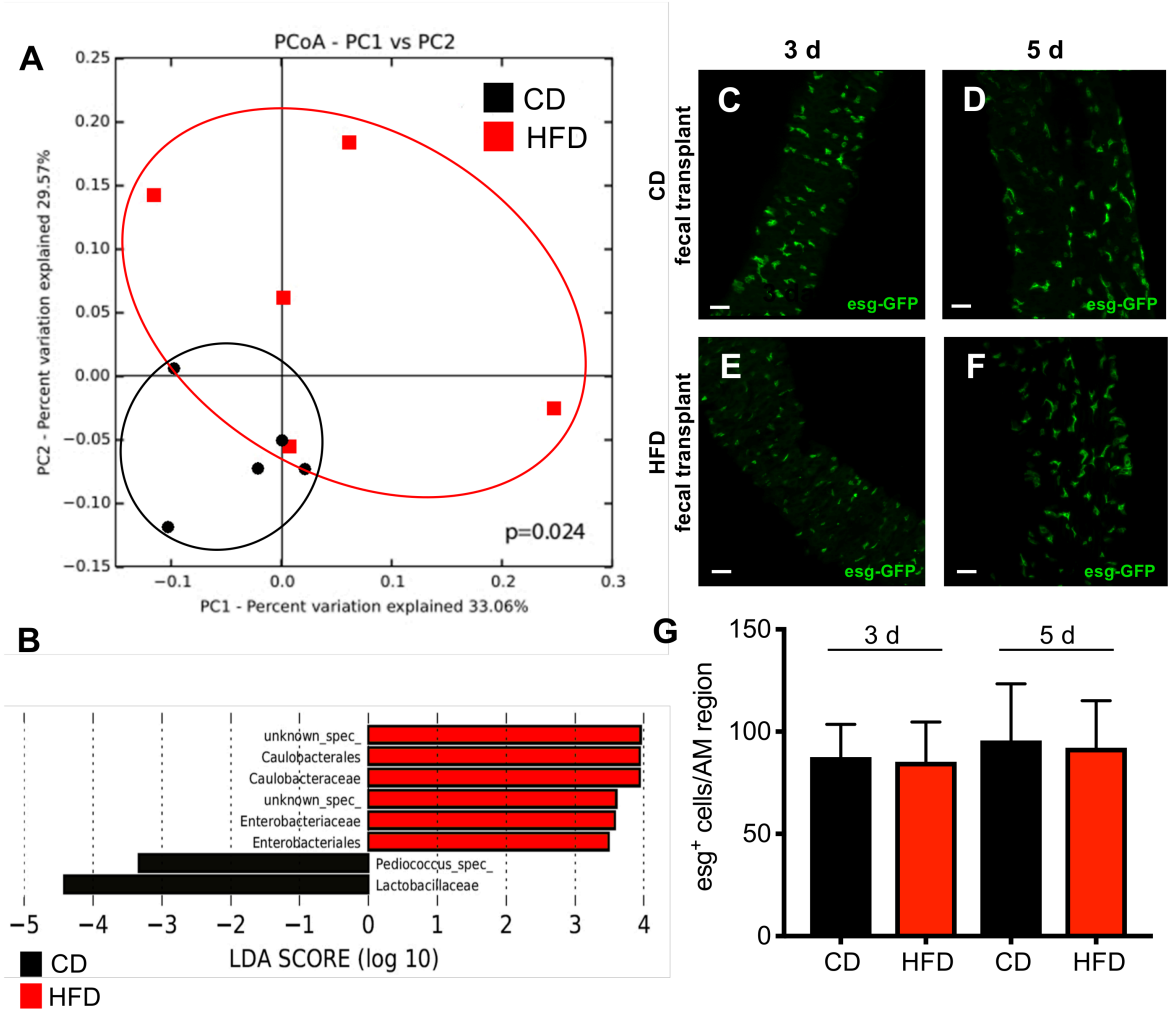

Figure 4. High fat diet alters the microbial composition of w^{1118} flies. (A) Principal coordinated analysis (PCoA) showed significant alterations of the intestinal microbiota community triggered by the diets. Each datapoint corresponds to one biological replicate. (B) Linear discriminant analysis effect size (LEfSe) determined differential enriched bacteria in the intestinal microbiota of the flies fed with a CD or HFD. Fecal transplant experiments into an *esg-Gal4::UAS-GFP* reporter strain was used to examine the effect of the diet induced altered microbial composition on the cell proliferation in the intestine (C-G). Animals reconstituted with a microbiota derived from animals on control diet (C, D) an those reconstituted with a microbiota derived from HFD treated animals (E, F) that were subjected either for 3 d (C, E) or 5 d (D, F) to these conditions. (G) Quantitative evaluation of the data shown in (C-F) (scale bar = 50µm, n = 8-12, ns = not significant, CD RC = control diet recolonized, HFD RC = high fat diet recolonized).

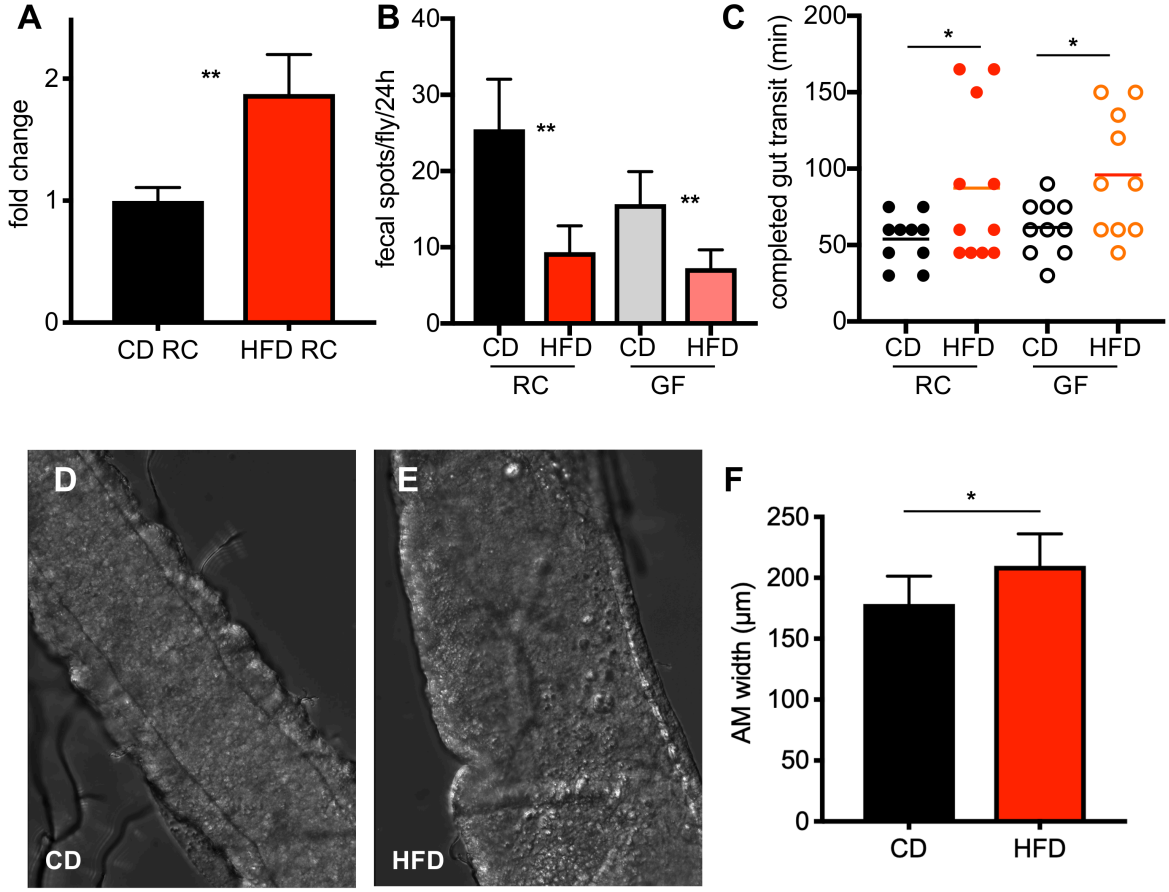

Figure 5. Impact of a high fat diet on egestion and microbial quantities. (A) The intestinal bacterial load was analyzed via qRT-PCR by using a 16S universal primers. The intestine were dissected 3 days after transferring the flies on either HFD or control diet (n =5). (B) Analysis of fecal spot production (24h period) flies with reconstituted microbiota or of germ free animals on control diet or on HFD (n = 7-10). (C) The transit time, defined as the time from food ingestion to egestion, was assessed by feeding blue colored food and observing the time until excretion of blue colored feces (n = 10). (D, E) Representative images of the R2 region after 3 days of control diet (D) or HFD (E, scale bar 50 µm). (F) Quantification of the intestinal thickness (n=10). CD RC = control diet recolonized, HFD RC = high fat diet recolonized, CD GF = control diet germ free, HFD GF = high fat diet germ free, *p>0.05, **p>0.01, ***p>0.001, ns = not significant.